HHS Public Access

Author manuscript

Cell Rep. Author manuscript; available in PMC 2018 October 28.

Published in final edited form as:

Cell Rep. 2018 May 22; 23(8): 2416–2428. doi:10.1016/j.celrep.2018.04.086.

Melanopsin Retinal Ganglion Cells Regulate Cone Photoreceptor Lamination in the Mouse Retina

Adele R. Tufford[1,2], **Jessica R. Onyak**[3], **Katelyn B. Sondereker**[3], **Jasmine A. Lucas**[4], **Aaron M. Earley**[4], **Pierre Mattar**[1,8], **Samer Hattar**[5], **Tiffany M. Schmidt**[4], **Jordan M. Renna**[3], and **Michel Cayouette**[1,2,6,7,9,*]

[1]Cellular Neurobiology Research Unit, Institut de Recherches Cliniques de Montréal, Montréal, QC, Canada

[2]Integrated Program in Neuroscience, McGill University, Montréal, QC, Canada

[3]Department of Biology, University of Akron, Akron, OH, USA

[4]Department of Neurobiology, Northwestern University, Evanston, IL, USA

[5]National Institute of Mental Health, Bethesda, MD, USA

[6]Department of Medicine, Universitéde Montréal, Montréal, QC, Canada

[7]Department of Anatomy and Cell Biology and Division of Experimental Medicine, McGill University, Montréal, QC, Canada

[8]Present address: Ottawa Hospital Research Institute and Department of Cellular and Molecular Medicine, University of Ottawa, Ottawa, ON, Canada

[9]Lead Contact

SUMMARY

Newborn neurons follow molecular cues to reach their final destination, but whether early life experience influences lamination remains largely unexplored. As light is among the first stimuli to reach the developing nervous system via intrinsically photosensitive retinal ganglion cells (ipRGCs), we asked whether ipRGCs could affect lamination in the developing mouse retina. We show here that ablation of ipRGCs causes cone photoreceptors to mislocalize at different apicobasal positions in the retina. This effect is partly mediated by light-evoked activity in ipRGCs, as dark rearing or silencing of ipRGCs leads a subset of cones to mislocalize.

*Correspondence: michel.cayouette@ircm.qc.ca.

AUTHOR CONTRIBUTIONS

Conceptualization, A.R.T. and M.C.; Investigation, A.R.T., J.R.O., K.B.S., J.A.L., and A.M.E.; Writing – Original Draft, A.R.T.; Writing – Review & Editing, P.M., T.M.S., S.H., J.M.R., and M.C.; Resources, T.M.S., S.H., J.M.R., and M.C.; Supervision, J.M.R., S.H., T.M.S., and M.C.; Funding Acquisition, M.C.

DECLARATION OF INTERESTS

The authors declare no competing interests.

DATA AND SOFTWARE AVAILABILITY

The accession number for the RNA sequencing data reported in this paper is GEO: GSE112404.

SUPPLEMENTAL INFORMATION

Supplemental Information includes Supplemental Experimental Procedures, eight figures, and four tables and can be found with this article online at https://doi.org/10.1016/j.celrep.2018.04.086

Furthermore, ablation of ipRGCs alters the cone transcriptome and decreases expression of the dopamine receptor D4, while injection of L-DOPA or D4 receptor agonist rescues the displaced cone phenotype observed in dark-reared animals. These results show that early light-mediated activity in ipRGCs influences neuronal lamination and identify ipRGC-elicited dopamine release as a mechanism influencing cone position.

In Brief

Tufford et al. show that light acting through intrinsically photosensitive retinal ganglion cells (ipRGCs) controls cone photoreceptor positioning in the developing mouse retina, using dopamine signaling as a cue. Ablation of ipRGCs disrupts cone positioning and induces changes in the cone transcriptome

Graphical Abstract

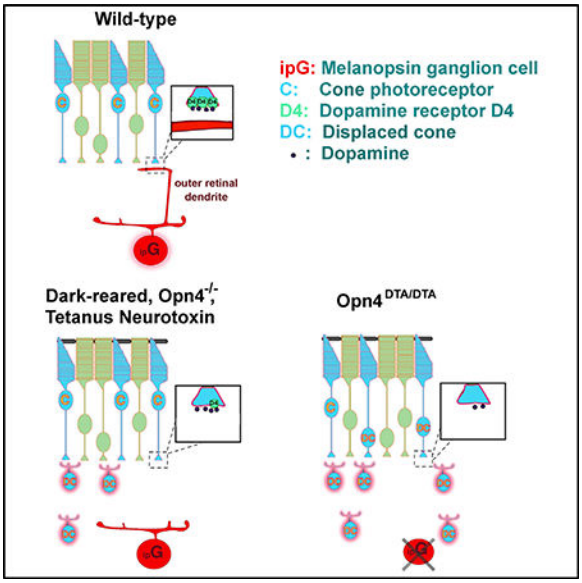

INTRODUCTION

The generation of functional neural circuits requires the integration of hard-wired cues with environmental experience, so that appropriate connections can be formed during development. A prerequisite for appropriate synaptic targeting is the proper laminar distribution of neurons, with defects in neuronal lamination often manifesting as profound perturbations in neural circuit assembly and function.

In the developing nervous system, activity and migratory cues converge to instruct the laminar destination of newly born neurons. Adhesive cues, such as the large secreted glycoprotein Reelin, act non-cell autonomously to instruct neuronal migration in various locations throughout the CNS (Tissir and Goffinet, 2003). Reelin signaling in turn converges on NMDA receptors to modulate the activity of cortical and hippocampal neurons (Chen et al., 2005; Sinagra et al., 2005). Correspondingly, glutamate-evoked activity is a potent cell-intrinsic regulator of lamination in cerebellar granule interneurons (Komuro and Rakic,

1993), cortical interneurons (De Marco García et al., 2011), and hippocampal interneurons (Manent et al., 2005). It remains unknown, however, whether experience-dependent activity has a role in neuronal lamination.

The neural retina represents a unique area of the CNS to address this question. Environmental light exposure can be easily manipulated during defined developmental time periods, and light reception can be controlled using well-established mouse mutants lacking photosensitivity. Importantly, readout of any neuronal lamination defects is facilitated by the welldefined architecture of the retina, consisting of 3 distinct neuronal layers containing stereotypical cell types. Rod and cone photoreceptors are both positioned in the outer nuclear layer (ONL), with cones further restricted to the apical-most part of the ONL. Next to the ONL is the inner nuclear layer (INL), which contains the cell bodies of signal-relay interneurons and Müller glial cells. Finally, the innermost ganglion cell layer€ (GCL) contains retinal ganglion cells (RGCs) and displaced amacrine interneurons. The recently discovered intrinsically photosensitive RGCs (ipRGCs), which also localize in the GCL, express the photo-pigment melanopsin and regulate photoentrainment and the pupillary light reflex (Güler et al., 2008€). Interestingly, ipRGCs have been recently described to send elaborate dendritic projections to the outer retina, which have been termed outer retinal dendrites (ORDs) (Renna et al., 2015; Sondereker et al., 2017).

Although several studies have used both dark-rearing and genetic approaches to demonstrate the importance of early activity in retinal synaptic targeting (Dunn et al., 2013; Kerschensteiner et al., 2009; Tian and Copenhagen, 2003), much less is known about how retinal cell bodies reach their appropriate layer. Specifically, whether light-evoked activity plays a role in this process remains unknown. As light is among the earliest environmental stimuli received by the CNS by way of ipRGCs, we hypothesized that ipRGCs could play a role in the lamination of the neural retina.

Using a combination of genetic ablation, dark rearing, and silencing of ipRGCs, we show here that ipRGCs regulate the lamination of cone photoreceptors in three dimensions: the laminar (apicobasal) axis, the pan-retinal dorsoventral (D/V) axis, and over time. Mechanistically, we provide evidence that ipRGC-elicited dopamine signaling functions as a cue for cone photoreceptor lamination. Together, this study demonstrates that ipRGCs regulate the laminar identity and distribution of a subset of cells within the mammalian retina, and it shows that sensory experience contributes to neuronal lamination in the CNS.

RESULTS

Developmental Ablation of ipRGCs Disrupts Cone Photoreceptor Lamination

Melanopsin-mediated photosensitivity is the earliest means of light detection in the mammalian retina (Rao et al., 2013; Sekaran et al., 2005; Tu et al., 2005), and it is thought to be the predominant means of photosensitivity prior to rod- and cone-driven light responses, which emerge just before eye opening at around post-natal day (P)8 and drive ganglion cells to spike as early as P10 (Bonezzi et al., 2018; Schmidt et al., 2008; Tian and Copenhagen, 2003). As ipRGCs send ORDs to the outer retina during the first 2 post-natal

weeks of life (Renna et al., 2015; Sondereker et al., 2017), we hypothesized that ipRGCs may be involved in organizing aspects of retinal architecture.

To test this idea, we ablated ipRGCs during development using animals expressing two copies of Diptheria-toxin A subunit in place of the melanopsin protein-coding locus (*Opn4*$^{DTA/DTA}$) (Chew et al., 2017). As recently described (Chew et al., 2017; Prigge et al., 2016), this mouse line achieves a near-complete ablation of ipRGCs during development, with ipRGC axons failing to invade the suprachiasmatic nucleus, and it shows no changes in number and morphology of various retinal cell types (Chew et al., 2017). We observed no obvious changes in the lamination of bipolar cells (Figure S1A), amacrine cells (Figure S1B), RGCs (Figure S1C), rod photoreceptors (Figures S2A and S2B), or horizontal cells (Figure S2C) in *Opn4*$^{DTA/DTA}$ retinas compared to wild-types. Additionally, we assessed the outer limiting membrane (OLM) integrity by staining for Crumbs1, an apical polarity protein critical for OLM maintenance and photoreceptor morphogenesis (Mehalow et al., 2003). Crumbs1 protein expression appeared unaffected in *Opn4*$^{DTA/DTA}$ retinas (Figure S2D).

To our surprise, however, we observed a disorganization of cone photoreceptor cells in *Opn4*$^{DTA/DTA}$ retinas at P7 and P16 (Figures 1A–1E). We observed many instances of short wavelength opsin (S-opsin) expressing cells outside of the ONL, in the INL and GCL of *Opn4*$^{DTA/DTA}$ animals (Figures 1A and 1B; Table S1). Co-staining with additional markers revealed that these displaced cells also expressed the classical cone photoreceptor markers Recoverin, Rxrγ, and cone arrestin (Figure S3A), as previously reported in the rat and human retina (Applebury et al., 2000), leading us to conclude that these cells are cone photoreceptors displaced to inappropriate retinal layers (hereafter referred to as displaced cones [DCs]). Many DCs also expressed long/medium wavelength opsin (LM-opsin) in addition to Sopsin, similar to the population of ONL cones (Applebury et al., 2000) (Figure S3B). As we failed to observe DCs expressing LM-opsin alone, S-opsin was used throughout our studies as a marker for the DC population. DCs were present as early as P0 in the wild-type retina, declining in number over the first 2 post-natal weeks, and they were retained in small numbers in the adult retina (Figure S3C).

DCs in the adult retina could be observed expressing synaptic markers Bassoon and PSD-95 in discrete puncta, suggesting they may engage in local circuitry (Figure S3D). Interestingly, DCs displayed a gradual change in their morphology over the course of the first 2 post-natal weeks, with the INL population progressing from more unipolar to more bipolar, with a concomitant increase in the proportion of multipolar morphologies (Figures S4A and S4B). Conversely, the GCL population showed a reduction in the proportion of bipolar morphologies over time, yet it showed a similar increase in multipolar morphologies over time (Figures S4A and S4B). The incidence of bipolar migratory-like morphologies among INL DCs as late as P14 was suggestive of continued migration. We hypothesized that the decline in the number of DCs over the first 2 post-natal weeks could be due to cell death. Consistently, we found DCs positive for Cleaved caspase-3 (CC3) in very rare instances in the P7 retina (Figure S4C).

Importantly, *Opn4*$^{DTA/DTA}$ animals also displayed a disruption of cone positioning *within* the ONL (Figures 1C–1E). Cone somas failed to properly align to the apical-most region, and they were found in significantly higher frequency in the basal 50% of the ONL compared to wild-type littermates (Figures 1C and 1D), while the total number of cone somas was unchanged (Figure 1E), excluding the possibility that cones localize basally by chance due to their increased frequency.

Interestingly, when we analyzed cone displacement early in post-natal development at P2, we observed no significant change in the number of DCs (Figures S5A and S5B), indicating that the phenotype arises later during the first post-natal week and is unlikely to be the result of earlier structural defects in the *Opn4*$^{DTA/DTA}$ retina. Importantly, the increase in DCs in the *Opn4*$^{DTA/DTA}$ retina remained in adult animals (>P60) (Figures 1F–1H), ruling out the possibility that the increase in DCs in the *Opn4*$^{DTA/DTA}$ retina simply reflects a delay in their developmental elimination and suggesting that ipRGCs are continuously required to restrict cones to the ONL.

Ablation of Melanopsin ipRGCs Alters the Cone Transcriptome

What could be the molecular mechanism by which ipRGCs regulate cone lamination? One possibility is that ipRGCs control the release of a signal that is perceived by cone photoreceptors as a cue to instruct their position. If so, we postulated that ablation of ipRGCs would lead to gene expression changes that could be used to identify the molecular cues involved. We therefore performed RNA sequencing on whole retinal extracts from P8 wild-type and *Opn4*$^{DTA/DTA}$ littermates. We sorted all reads into the retinal cell type-specific profiles defined using Drop sequencing (Drop-seq) analysis of single retinal cells (Macosko et al., 2015) (Figure 2A). Interestingly, ipRGC ablation resulted in minor overall expression changes in most cell types at P8, with the notable exception of genes expressed in cone photoreceptors, and the expected downregulation of melanopsin (Opn4) in RGCs (Figures 2A–2C; Table S2). A Database of Annotation, Visualization, and Integrated Discovery (DAVID) analysis of highly downregulated genes revealed that the two most highly affected gene groups were those involved in photosensitivity and sensory perception (Figure 2D). Notably, P8 *Opn4*$^{DTA/DTA}$ animals exhibited a significant increase in cone arrestin expression, which would result in reduced activation of the cone phototransduction cascade. These results indicate that ipRGCs influence cone-specific gene expression during the first postnatal week, including genes related to cone activity.

Light Regulates Cone Lamination during Retinal Development

Our observation of reduced expression of cone phototransduction cascade genes in the P8 *Opn4*$^{DTA/DTA}$ retina was suggestive of an alteration in early cone activity. To investigate the activitydependent contribution from ipRGCs to cone photoreceptor lamination, we deprived animals of all light input during development and surveyed for changes in cone photoreceptor positioning. We reared wild-type C57BL/6J pregnant dams in constant total darkness (DD) starting from embryonic day (E) 13.5, and we sacrificed pups post-natally. Interestingly, DCs always appeared more abundant in DD animals at all ages examined (Figures 3A and 3B), consistent with the possibility that light might play a role in the developmental lamination of cones. Total dark rearing resulted in a significant increase in

the number of DCs per unit retina at P7, P14, and P21 compared to 12-hr light/12-hr dark (LD) controls (Figures 3C and 3D; Table S1). Dark rearing pups during the embryonic period only (E13–P0,DD-embryonic) failed to elicit a significant increase in the number of DCs, whereas dark rearing pups during the post-natal period only (P0 onward, DD-post-natal) recapitulated the effect of total dark rearing until P7 (Figure 3C). Additionally, dark rearing pups from E13 to P7, followed by a transition into 7 days of LD until P14, failed to reduce the number of DCs back to control levels (Figure 3C), and rearing pups in LD until P7 followed by DD until P16 did not significantly increase the number of DCs (Figure 3C). Importantly, cone lamination within the ONL was not affected by dark rearing, suggesting that light-independent mechanisms control this aspect of cone positioning. Finally, we observed no obvious changes in bipolar cell, amacrine cell, or RGC laminar position in DD pups compared to control pups reared on a standard LD cycle, similar to the P8 *Opn4*$^{DTA/DTA}$ retina (Figures S6A–S6C). Together, these results indicate that light acts primarily during the first post-natal week to restrict cone somas to the photoreceptor layer.

Cone Lamination Is Controlled by Activity in ipRGCs Independently of Early Cone Activity

Dark rearing could conceivably affect early cone activity directly, in addition to ipRGC activity. S-opsin expression is detectable as early as E15.5 (Aavani et al., 2017), but it is believed that immature cones (i.e., before P8) do not functionally respond to light due to their lack of outer segments and underdeveloped ribbon synapse (Bakall et al., 2003; Bonezzi et al., 2018; Rich et al., 1997). To directly test whether light was acting through ipRGCs to influence cone lamination, we manipulated early photosensitivity independently in cones and ipRGCs using genetic approaches. In *Cnga3*$^{-/-}$mice, which lack the ion channel necessary for light-evoked activity in cones, we observed no significant increase in the number of DCs at P7 (Figures 4A and 4B; Table S1), although a trend toward an increase was observed, perhaps reflecting early degeneration in the *Cnga3*$^{-/-}$ retina leading to cellular detachment, as previously described (Biel et al., 1999). In contrast, in mice lacking the ipRGC photopigment melanopsin (*Opn4*$^{-/-}$), we observed a significant increase in the number of DCs compared to wild-type littermates at P7 (Figures 4C and 4D; Table S1). Comparing the two manipulations directly, *Opn4*$^{-/-}$ retinas had significantly more DCs than *Cnga3*$^{-/-}$ retinas ($p = 0.0082$, Student's t test). As in DD animals, we observed no obvious change in cone position within the ONL or any gross morphology or lamination defects of bipolar cells, amacrine cells, or RGCs in P7 *Opn4*$^{-/-}$animals (Figures S7A and S7B) and no change in the total number of Brn3b-expressing RGCs (Figure S7C), excluding the possibility that a loss of melanopsin affects other early born cell types. Interestingly, by the time rod and cone photoreceptors are able to drive light responses in ipRGCs around P11 (Schmidt et al., 2008), we observed a rescue in the number of DCs back to wild-type levels in the *Opn4*$^{-/-}$ mice (Figures 4C and 4D). Together these results indicate that, during the first post-natal week, photosensation in ipRGCs influences cone lamination.

To address whether neurosecretion in ipRGCs is required for cone lamination, we generated animals expressing Tetanus Neurotoxin (TeNT) in ipRGCs by crossing a mouse line expressing Cre-recombinase in place of the melanopsin proteincoding gene (*Opn4*^{Cre}) with Cre-dependent TeNT-expressing animals (*Rosa*$^{TeNT/+}$). TeNT blocks neurotransmitter release by cleaving VAMP/Synaptobrevin-2, thereby abolishing classical neurosecretion

(Schiavo et al., 1992; Zhang et al., 2008b). Interestingly, we observed a significant increase in the number of DCs outside the ONL in *Opn4*$^{Cre/+}$; *Rosa*$^{TeNT/+}$ animals at P14 compared to controls (Figures 4E and 4F; Table S1), indicating that ipRGC-mediated neurosecretion is required to restrict at least a subset of cones to the ONL into the second post-natal week. As we failed to observe a change in the number of DCs at P7 in *Opn4*$^{Cre/+}$; *Rosa*$^{TeNT/+}$ retinas (Figures 4E and 4F), most likely due to inefficient or insufficient TeNT expression during the first post-natal week from only one copy of TeNT, we next sought to examine mice wherein the majority of RGCs express Cre from E15.5 (*Isl1*^{Cre}; *Rosa*$^{TeNT/tdTomato}$) (Elshatory et al., 2007). In this mouse line, we confirmed that all ipRGCs visible at P7 by melanopsin immunostaining were also positive for the tdTomato reporter in *Isl1*$^{Cre/+}$; *Rosa*$^{TeNT/tdTomato}$ animals (Figure 4G, inset). As predicted, we observed a significant increase in the number of DCs in P7 *Isl1*$^{Cre/+}$; *Rosa*$^{TeNT/tdTomato}$ animals compared to Cre-negative littermate controls (Figures 4G and 4H; Table S1). Together with our observation that post-natal dark rearing alone results in an increase in the number of DCs (Figure 3C), these results support a model wherein neurosecretion from ipRGCs actively influences cone lamination within the first 2 post-natal weeks of life.

Melanopsin ORDs Are in an Opposing Gradient to DC Photoreceptors

How could ipRGCs residing in the inner retina influence the lamination of cones residing in the outer retina? A recently described subset of M1-subtype ipRGCs possesses an ORD, which projects all the way to the outer plexiform layer (OPL) to contact cone terminals during post-natal development (Renna et al., 2015; Sondereker et al., 2017) (Figures 5A and 5B). ipRGC ORDs arise from M1 ipRGCs in both the GCL (M1) and INL(M1d), are anatomically distinct from the ipRGC axon collateral, and are located preferentially in the dorsal hemisphere of the retina (Sondereker et al., 2017). Importantly, ORDs were shown to elaborate and mature between P4 and P8, peaking numeri-cally at P12 (Renna et al., 2015; Sondereker et al., 2017), which mirrors the timeline for cone lamination.

Remarkably, we found that total dark rearing resulted in a decrease in the total number of ipRGC ORDs at P8, P12, and P30 (Figure 5C; Table S3), in contrast to our observed effect on DCs (Figure 3C). Moreover, by examining the gradient of ipRGC ORDs and DCs within the same retina at P8, we found that ORDs and DCs preferentially occupy separate retinal compartments, with ORDs located predominantly dorsally and DCs located predominantly ventrally (Figures 5D–5F; Table S3). Strikingly, dark rearing resulted in a significant shift in the distribution of both populations (Figures 5D–5F; Table S3). We observed no change in the length of existing M1- and M1d-originating ORDs in dark-reared animals relative to light-reared controls at P8 (Figure 5G; Table S3), as well as no significant change in their number of dendritic branch points (Figure 5H; Table S3). This indicates that light regulates the overall number of ORDs, possibly at the level of outgrowth from the cell soma, but not the growth and complexity of ORDs during the first post-natal week.

If the presence of ORDs is required to maintain appropriate cone lamination, we predicted that ablation of ipRGCs would disrupt the D/V distribution of DCs. Consistently, we observed a near randomization of DCs in *Opn4*$^{DTA/DTA}$ animals at P7 (Figures 5I and 5J;

Table S3). Together, these observations suggest that ipRGCs may use their ORDs to communicate with cone photoreceptors to regulate the number of DCs.

D4-Mediated Dopamine Signaling Influences Cone Photoreceptor Positioning

To explain how ipRGCs could regulate cone positioning, we examined potential changes in signaling or secreted molecules from our RNA sequencing analysis. Among the significantly altered transcripts in P8 *Opn4*$^{DTA/DTA}$ versus wild-type retinas, the dopamine receptor D_4 (Drd4) appeared to be a good candidate, showing significantly reduced expression (Figure 2B). DRD4 expression was confirmed to be expressed in cones in four separate transcriptional datasets (Hughes et al., 2017; Kim et al., 2016; Mo et al., 2016; Siegert et al., 2012). In the mature retina, ipRGCs are known to influence cone photoreceptor light adaptation by controlling dopamine (DA) release from dopaminergic amacrine cells (DACs) (Prigge et al., 2016; Zhang et al., 2008a), an effect dependent on the expression of DRD4 (Jackson et al., 2012).

Interestingly, we observed many instances of ipRGC ORDs coalescing with DAC dendrites in the outer retina, directly adjacent to cone pedicles (Figures S8A–S8C). When quantified in serial sections, 28.5% ± 14.3% of tomato-expressing presumptive ORDs from P8 *Opn4*$^{Cre/+}$ × *Rosa*^{tdTomato} co-localized with tyrosine hydroxylase (TH)-positive processes in the outer plexiform layer, whereas 40.2% ± 6.6% of ORDs terminating in the INL co-localized with TH-positive processes (Figure S8C). Together with our observation of reduced *Drd4* expression in the *Opn4*$^{DTA/DTA}$ retina, these results were consistent with the possibility that ipRGC ORDs may lead to DA release from DACs, providing a positional cue to cones via DRD4 signaling.

To test this idea, we utilized an *in vitro* paradigm of cultured retinal explants, wherein RGCs undergo large-scale apoptosis within the first several days (Manabe et al., 2002). Interestingly, in retinal explants cultured for 7 days, we found that cone photoreceptors readily displaced to the explant INL and also displayed a dramatic disruption of their cell bodies within the explant ONL, in a manner reminiscent of the *Opn4*$^{DTA/DTA}$ phenotype (Figures 6A and 6G). Daily supplementation of explant cultures with 1 or 10 μM DA resulted in a drastic decrease in the number of DCs (Figures 6B, 6C, and 6G), suggesting that DA-evoked activity in cones may act as a cue to restrict cones to their appropriate layer. To address whether DA acts via DRD4, we supplemented explant cultures with the selective DRD4 agonist A412997 (Browman et al., 2005), and we found that daily supplementation of 10 μM A412997 or a combination of 1 μM DA and 1 μM A412997 also significantly reduced the number of DCs (Figures 6E–6G), while 1 μM A412997 alone was not sufficient to rescue cone position (Figures 6D and 6G). In contrast, we failed to observe significant changes in rod photoreceptor cell positioning in explant manipulations (Figures 6H–6K), leading us to conclude that this effect was specific to cones.

Should a reduction in DRD4-mediated signaling to cones be the cause of lamination defects observed in our different in vivo manipulations, we reasoned that administration of exogenous sources of DA or DRD4 agonists should rescue the phenotypes. As predicted, *in vivo* subcutaneous administration of the DA precursor L-DOPA or the DRD4 agonist A412997 in DD animals was able to bring the number of DCs back to that of LD controls

(Figures 7A–7E; Table S1). These observations suggest that DA signaling, likely released by DAC dendrites and acting on the cone via DRD4, influences cone positioning in the developing retina.

DISCUSSION

The process of neuronal lamination in the CNS often involves the recruitment of players already present in the developing circuit to guide newly born neurons (Marín and Rubenstein, 2003; Tissir and Goffinet, 2003). In an area of the CNS designed to detect and interpret changes in light exposure, it appears logical that early born ipRGCs would use optical stimuli to guide the lamination of other cell types in the retina. Our study now provides support for this idea.

ipRGCs Shape Cone Photoreceptor Territories

During early stages of retinogenesis, the newborn cone extends processes that span the nascent ONL, and the soma moves basally to make way for the subsequent waves of neurogenesis (Weber et al., 2014). After neurogenesis, cones are one of the last retinal cell types to take on their mature position, reaching the apical-most compartment of the ONL around the time of eye opening. An external mechanism must, therefore, restrict cone soma position during a time of rapid and substantial circuit remodeling. Recently, it was shown that impairment in the apical membrane of the ONL during development results in an increase in ectopic cone photoreceptors in the sub-retinal compartment (Jimeno et al., 2016). This study highlights a structural feature of the retina that prevents cones from migrating too far apically, but it leaves the question of what could restrict cones from migrating too far basally within the neural retina proper. A small sub-population of cones displaced to the inner retina has been previously reported in the rat and human retina (Semo et al., 2007), consistent with the findings reported here in mice. Similarly, a small population of displaced rod photoreceptors has been observed in the rat retina, but these cells appear to be eliminated by adulthood (Gunhan et al., 2003; Szabo€ ´ et al., 2014). In contrast, our data indicate that at least some DCs remain in the adult mouse retina and the continued presence of ipRGCs is required to restrict their numbers, as evidenced by the elevated number of DCs in adult *Opn4*$^{DTA/DTA}$ retinas compared to controls.

Considering that dark rearing or silencing of ipRGCs leads to the mispositioning of a subset of cones to the inner layers without affecting cone lamination within the ONL, whereas total ablation of ipRGCs disrupts both aspects of cone positioning, we propose that ipRGCs might use contact-dependent cues or perhaps play a structural support role, in addition to light-evoked DRD4 signaling, to regulate cone lamination. Given that some cones remain normally positioned, even after ablation of ipRGCs, it is likely that as-yet unidentified ipRGC-independent factors contribute to cone lamination.

In the mature retina, M1-ipRGCs send axon collaterals within the inner plexiform layer to release glutamate onto DACs, regulating their DA release, which in turn modulates cone light adaptation via action on DRD4 (Joo et al., 2013; Prigge et al., 2016; Zhang et al., 2008a). Whereas ipRGC axon-collateral-mediated DA release in the mature retina would likely result in widespread DAC activation, the presence of asymmetrically distributed

ipRGC ORDs in the developing post-natal retina likely results in DA release from DACs preferentially in the dorsal retina, which could act as a more precise mechanism of cone lamination throughout time and space. DA release from DACs is likely diffusion limited, raising the possibility that DCs in wild-type animals could be the result of gaps in available DA in the outer plexiform layer. DA release need not be changed in our manipulations, however; our observed phenotypes could be solely the result of reduced DRD4 expression, with ipRGCs communicating with cones directly to regulate DRD4 expression and DA reception.

Nevertheless, neurosecretion from dendrites is a well-established concept in the CNS, particularly in neuropeptide-secreting cells (Kennedy and Ehlers, 2011), making it likely that activity in ipRGCs results in dendritic neurotransmitter secretion, which may influence DA release from DACs. As manipulations of neurotransmitter release specifically from dendritic or axonal compartments is not feasible *in vivo*, we cannot exclude the possibility that a few ipRGC axon collaterals contribute to DAC input and DA release. However, given the strong and inverse correlation in space and time between ipRGC ORDs and DCs, our observation of coalescing ipRGC and DAC dendrites (Figure S8, the inverse responses of ORDs and DCs to light deprivation, and the significantly altered DC distribution in Opn4DTA/DTA, we favor a model wherein ORDs activate DACs, which could in turn secrete DA locally to influence cone lamination via DRD4mediated signaling (Figures 7F–7H).

DA Signaling as a Cue for Cone Photoreceptor Position

How could DA affect cell positioning at the level of individual cones? DA signaling to cones is known to influence cone activity (Jackson et al., 2012; Prigge et al., 2016), and it is presumed to result in increased intracellular Ca^{2+} in the cone. Decreased levels of retinal DA have been reported in mice reared from birth on a short photoperiod (Jackson et al., 2014). Decreased input from ipRGCs and a concomitant decrease in DA release from DACs may trigger compensatory pathways in cones involving proteins typically used to control intracellular Ca^{2+}, as evidenced by our observed transcriptional changes in phototransduction genes in *Opn4*$^{DTA/DTA}$ retinas. DA signaling has also been shown to affect cellular migration of cortical GABA-ergic interneurons by modulating the cytoskeleton (reviewed in Money and Stanwood, 2013). Calcium-mediated cyclic AMP (cAMP) and protein kinase A (PKA) activation is a well-established pathway by which Ca^{2+} fluxes regulate cytoskeletal remodeling and cellular migration during neuronal lamination (Toriyama et al., 2012). The nucleoskeleton-to-cytoskeleton linker complexes (LINCs) required for cone-specific cell positioning have been described (Razafsky et al., 2012; Yu et al., 2011), although whether they are disrupted when cone activity changes has yet to be demonstrated.

Light as a Cue for Neuronal Lamination

Light is among the first environmental stimuli during development. Prior to birth, light reaches through the uterine cavity of a pregnant dam in sufficient amounts to drive melanopsin photoreception, controlling the regression of the neonatal hyaloid vasculature (Rao et al., 2013). The amount of light permeating the eyelid in a post-natal pup is,

therefore, thought to be sufficient to drive light-evoked responses in ipRGCs, which are an important regulator of early post-natal retinal waves (Renna et al., 2011). Indeed, we demonstrate here a previously unsuspected role for light-evoked experience in the regulation of dendrite outgrowth, as evidenced by the changes in the number of melanopsin ORDs observed in DD animals. We cannot rule out the possibility that light may act via additional mechanisms to influence cone photoreceptor positioning during development, including but not limited to *Opn5*/neuropsin-mediated photosensitivity (Buhr et al., 2015), or secondary effects of ipRGC silencing/light deprivation, such as altered retinal wave properties (Chew et al., 2017; Renna et al., 2011).

The effects of visual deprivation on retinal development have not been extensively studied, and much remains to be described. To ascertain a potential functional consequence of inappropriate cone lamination, we attempted to measure photoreceptor electroretinography (ERG) responses at early developmental time points, when our phenotypes are most severe. However, the immature cone photoreceptor ERG prevented us from reaching any conclusions (data not shown). At the level of the individual cone, however, the consequence of inappropriate lamination is most likely cell death; the vast majority of DCs appears to be eliminated by adulthood. ipRGCs may restrict cones to their appropriate layer to ensure appropriate synaptic targeting and survival.

Nevertheless, several studies point to a potential functional consequence of visual deprivation lasting until adulthood. Developmental dark rearing results in a suppression of the inner retinal light response in the adult mouse retina (Tian and Copenhagen, 2001), attributed to a disruption in the refinement of on-off RGC dendritic lamination in the inner plexiform layer (Tian and Copenhagen, 2003). In humans, patients affected by total congenital cataract before 6 months of age show a 30%–35% decrease in cone-driven retinal function versus healthy controls up to 9 years following surgical removal of cataracts (Esposito Veneruso et al., 2017). Low light exposure during human gestation, as observed in northern climates, has also been shown to strongly correlate with the incidence of retinopathy of prematurity (Yang et al., 2013). Understanding the impacts of early light exposure may lead to novel treatments for multiple light-related disorders.

EXPERIMENTAL PROCEDURES

See Table S4 for reagents and sources.

Mice

All experiments were carried out in accordance with Canadian Council on Animal Care guidelines and NIH guidelines for laboratory animal use. Wild-type C57BL/6J mice, *Cnga3*$^{-/-}$ mice, and *Isl1*^{Cre} mice were obtained from Jackson ImmunoResearch Laboratories. Rosa-TeNT mice were generously provided by Martyn Goulding (Zhang et al., 2008b). All other lines were generated by the authors and maintained on a mixed C57BL/6J/129S1 background. PCR genotyping for *Opn4*$^{LacZ/LacZ}$, *Opn4*^{Cre}, and *Opn4*^{DTA} lines was carried out as published (Chen et al., 2013; Hattar et al., 2002; Prigge et al., 2016). Both male and female animals were used at the indicated developmental and adult time points.

Dark Rearing

Timed-pregnant females were placed in complete and constant darkness from E13.5 onward, and pups were sacrificed at 7, 14, or 21 days age. LD controls were maintained on a 12:12 light:dark cycle with ambient light-phase intensity averaging 200 lux.

Retinal Explant Cultures

Retinal explants were prepared from P0 pups as previously described (Cayouette et al., 2003). DA-HCl and/or A412997 (Tocris) were diluted in media and added to culture media daily. Explants were fixed in 4% paraformaldehyde on day 7 and processed for histology (below).

Subcutaneous Drug Administration

Neonatal pups were administered 20 μg L-DOPA (Tocris) subcutaneously in 20 μL Hank's balanced salt solution (HBSS) daily between the ages of P2 and P6. For A412997 (Tocris), pups were administered 38 ng in 20 μL HBSS daily between the ages of P3 and P6.

RNA Sequencing

Opn4$^{DTA/+}$ male and female mice were mated to produce *Opn4*$^{+/+}$ and *Opn4*$^{DTA/DTA}$ littermates. Retinal RNA was extracted using a QIAGEN RNAeasy kit. Directional mRNA libraries were prepared using the Illumina TruSeq mRNA kit. Samples were converted to a cDNA library by reverse transcription, amplified by PCR, and sequenced on the Illumina HiSeq2500. Reads were aligned to the *Mus musculus* genome (mm10). Differential expression was determined using DESeq2. The cutoff for determining significantly differentially expressed genes was a false discovery rate (FDR)-adjusted p value less than 0.05. The RNA-seq dataset was deposited to NCBI GEO: GSE112404. See the Supplemental Experimental Procedures for details and references.

Histology

Immunohistochemistry on retinal sections and whole mounts was performed as per Chew et al. (2017) and Sondereker et al. (2017), with modifications and antibodies as described in detail in the Supplemental Experimental Procedures and Table S4. Whole-mount retinas were imaged in piecemeal at low magnification and then manually stitched together to form a complete reconstruction of the retina.

Quantification and Statistical Analysis

Quantifications are reported as mean ± SEM. Statistical tests are Student's t tests or one-way ANOVA with Tukey post-test. The p values reported in each figure legend are labeled as follows: *$p < 0.05$, **$p < 0.01$, and ***$p < 0.001$. Reported 'n' represents the number of independent animals except where noted.

DC counts were measured from 20-μm histological sections of whole retinas, sectioned through the entire width of the eye. Every fifth section of the entire retina was stained for S-opsin, allowing the number of DCs in both the INL and GCL to be counted in the entire length of one section per 100 mm retina, which was then averaged across the entire retina.

Average DCs per section thus denotes the average number of INL and GCL S-opsin-expressing cells per histological section. DCs in retinal explants were calculated by measuring the number of S-opsin somas displaced to the INL or GCL within 400 μm measured segments from ~20 images per condition, per replicate. Each replicate is one independent experiment consisting of a minimum of two retinas from two separate animals per condition.

Displaced ONL cones in wild-type and *Opn4*$^{DTA/DTA}$ retinas were quantified as follows: every tenth section through the entire retina was collected and stained for S-opsin, two images were taken from either edge of the section (roughly 25% and 75% distance along the length of the section), and the total number of cone somas versus the number of cones displaced 50% basally within the ONL within a 100-μm segment in each image was counted.

ORDs were quantified as previously described (Sondereker et al., 2017), and they are described as the total number of ORDs per retina. See the Supplemental Experimental Procedures for a detailed description.

Supplementary Material

Refer to Web version on PubMed Central for supplementary material.

ACKNOWLEDGMENTS

We wish to thank B. Day, M.C. Lavallé e, and J. Barthe for mouse care; M. Goulding for the *Rosa*^{TeNT} mice; E. Ruthazer, K. Murai, and G. Awatramani for critical insight on the project; and members of the Cayouette lab for support. This work was supported by grants from the Foundation Fighting Blindness Canada and the Canadian Institutes of Health Research (CIHR 77570). A.R.T. was supported by a CIHR Canada Graduate Scholarship. M.C. holds the Gae¨ tane and Roland Pillenié re Chair in Retina Biology and is an Emeritus Research Scholar from the Fonds de la Recherche – Qué bec (FRQS). Additional support to J.M.R. was provided by the NIH (R15EY026255–01) and The Karl Kirchgessner Foundation.

REFERENCES

Aavani T, Tachibana N, Wallace V, Biernaskie J, and Schuurmans C (2017). Temporal profiling of photoreceptor lineage gene expression during murine retinal development. Gene Expr. Patterns 23–24, 32–44. [PubMed: 28288836]

Applebury ML, Antoch MP, Baxter LC, Chun LL, Falk JD, Farhangfar F, Kage K, Krzystolik MG, Lyass LA, and Robbins JT (2000). The murine cone photoreceptor: a single cone type expresses both S and M opsins with retinal spatial patterning. Neuron 27, 513–523. [PubMed: 11055434]

Bakall B, Marmorstein LY, Hoppe G, Peachey NS, Wadelius C, and Marmorstein AD (2003). Expression and localization of bestrophin during normal mouse development. Invest. Ophthalmol. Vis. Sci 44, 3622–3628. [PubMed: 12882816]

Biel M, Seeliger M, Pfeifer A, Kohler K, Gerstner A, Ludwig A, Jaissle G, Fauser S, Zrenner E, and Hofmann F (1999). Selective loss of cone function in mice lacking the cyclic nucleotide-gated channel CNG3. Proc. Natl. Acad. Sci. USA 96, 7553–7557. [PubMed: 10377453]

Bonezzi PJ, Stabio ME, and Renna JM (2018). The development of mid-wavelength photoresponsivity in the mouse retina. Curr. Eye Res 43, 666–673. [PubMed: 29447486]

Browman KE, Curzon P, Pan JB, Molesky AL, Komater VA, Decker MW, Brioni JD, Moreland RB, and Fox GB (2005). A-412997, a selective dopamine D4 agonist, improves cognitive performance in rats. Pharmacol. Biochem. Behav 82, 148–155. [PubMed: 16154186]

Buhr ED, Yue WWS, Ren X, Jiang Z, Liao H-W, Mei X, Vemaraju S, Nguyen M-T, Reed RR, Lang RA, et al. (2015). Na. Proc. Natl. Acad. Sci. USA 112, 13093–13098.

Cayouette M, Barres BA, and Raff M (2003). Importance of intrinsic mechanisms in cell fate decisions in the developing rat retina. Neuron 40, 897–904. [PubMed: 14659089]

Chen Y, Beffert U, Ertunc M, Tang T-S, Kavalali ET, Bezprozvanny I, and Herz J (2005). Reelin modulates NMDA receptor activity in cortical neurons. J. Neurosci 25, 8209–8216. [PubMed: 16148228]

Chen S-K, Chew KS, McNeill DS, Keeley PW, Ecker JL, Mao BQ, Pahlberg J, Kim B, Lee SCS, Fox MA, et al. (2013). Apoptosis regulates ipRGC spacing necessary for rods and cones to drive circadian photoentrainment. Neuron 77, 503–515. [PubMed: 23395376]

Chew KS, Renna JM, McNeill DS, Fernandez DC, Keenan WT, Thomsen MB, Ecker JL, Loevinsohn GS, VanDunk C, Vicarel DC, et al. (2017). A subset of ipRGCs regulates both maturation of the circadian clock and segregation of retinogeniculate projections in mice. eLife 6, e22861–e22873. [PubMed: 28617242]

De Marco García NV, Karayannis T, and Fishell G (2011). Neuronal activity is required for the development of specific cortical interneuron subtypes. Nature 472, 351–355. [PubMed: 21460837]

Dunn FA, Della Santina L, Parker ED, and Wong RO (2013). Sensory experience shapes the development of the visual system's first synapse. Neuron 80, 1159–1166. [PubMed: 24314727]

Elshatory Y, Deng M, Xie X, and Gan L (2007). Expression of the LIM-homeodomain protein Isl1 in the developing and mature mouse retina. J. Comp. Neurol 503, 182–197. [PubMed: 17480014]

Esposito Veneruso P, Ziccardi L, Magli G, Parisi V, Falsini B, and Magli A (2017). Early light deprivation effects on human cone-driven retinal function. Acta Ophthalmol. 95, 133–139. [PubMed: 27535202]

Gu€ler, AD, Ecker JL, Lall GS, Haq S, Altimus CM, Liao H-W, Barnard AR, Cahill H, Badea TC, Zhao H, et al. (2008). Melanopsin cells are the principal conduits for rod-cone input to non-image-forming vision. Nature 453, 102–105. [PubMed: 18432195]

Gu€nhan E, van der List D, and Chalupa LM (2003). Ectopic photoreceptors and cone bipolar cells in the developing and mature retina. J. Neurosci. 23, 1383–1389. [PubMed: 12598626]

Hattar S, Liao H-W, Takao M, Berson DM, and Yau K-W (2002). Melanopsin-containing retinal ganglion cells: architecture, projections, and intrinsic photosensitivity. Science 295, 1065–1070. [PubMed: 11834834]

Hughes AEO, Enright JM, Myers CA, Shen SQ, and Corbo JC (2017). Cell Type-Specific Epigenomic Analysis Reveals a Uniquely Closed Chromatin Architecture in Mouse Rod Photoreceptors. Sci. Rep 7, 43184. [PubMed: 28256534]

Jackson CR, Ruan G-X, Aseem F, Abey J, Gamble K, Stanwood G, Palmiter RD, Iuvone PM, and McMahon DG (2012). Retinal dopamine mediates multiple dimensions of light-adapted vision. J. Neurosci. 32, 9359–9368. [PubMed: 22764243]

Jackson CR, Capozzi M, Dai H, and McMahon DG (2014). Circadian perinatal photoperiod has enduring effects on retinal dopamine and visual function. J. Neurosci 34, 4627–4633. [PubMed: 24672008]

Jimeno D, Go´ mez C, Calzada N, de la Villa P, Lillo C, and Santos E. (2016). RASGRF2 controls nuclear migration in postnatal retinal cone photoreceptors. J. Cell Sci 129, 729–742. [PubMed: 26743081]

Joo HR, Peterson BB, Dacey DM, Hattar S, and Chen S-K (2013). Recurrent axon collaterals of intrinsically photosensitive retinal ganglion cells. Vis. Neurosci 30, 175–182. [PubMed: 23834959]

Kennedy MJ, and Ehlers MD (2011). Mechanisms and function of dendritic exocytosis. Neuron 69, 856–875. [PubMed: 21382547]

Kerschensteiner D, Morgan JL, Parker ED, Lewis RM, and Wong ROL (2009). Neurotransmission selectively regulates synapse formation in parallel circuits in vivo. Nature 460, 1016–1020. [PubMed: 19693082]

Kim J-W, Yang H-J, Oel AP, Brooks MJ, Jia L, Plachetzki DC, Li W, Allison WT, and Swaroop A (2016). Recruitment of Rod Photoreceptors from Short-Wavelength-Sensitive Cones during the Evolution of Nocturnal Vision in Mammals. Dev. Cell 37, 520–532. [PubMed: 27326930]

Komuro H, and Rakic P (1993). Modulation of neuronal migration by NMDA receptors. Science 260, 95–97. [PubMed: 8096653]

Macosko EZ, Basu A, Satija R, Nemesh J, Shekhar K, Goldman M, Tirosh I, Bialas AR, Kamitaki N, Martersteck EM, et al. (2015). Highly Parallel Genome-wide Expression Profiling of Individual Cells Using Nanoliter Droplets. Cell 161, 1202–1214. [PubMed: 26000488]

Manabe S, Kashii S, Honda Y, Yamamoto R, Katsuki H, and Akaike A (2002). Quantification of axotomized ganglion cell death by explant culture of the rat retina. Neurosci. Lett 334, 33–36. [PubMed: 12431769]

Manent JB, Demarque M, Jorquera I, Pellegrino C, Ben-Ari Y, Aniksztejn L, and Represa A (2005). A noncanonical release of GABA and glutamate modulates neuronal migration. J. Neurosci 25, 4755–4765. [PubMed: 15888651]

Marín O, and Rubenstein JLR. (2003). Cell migration in the forebrain. Annu. Rev. Neurosci 26, 441–483. [PubMed: 12626695]

Mehalow AK, Kameya S, Smith RS, Hawes NL, Denegre JM, Young JA, Bechtold L, Haider NB, Tepass U, Heckenlively JR, et al. (2003). CRB1 is essential for external limiting membrane integrity and photoreceptor morphogenesis in the mammalian retina. Hum. Mol. Genet 12, 2179–2189. [PubMed: 12915475]

Mo A, Luo C, Davis FP, Mukamel EA, Henry GL, Nery JR, Urich MA, Picard S, Lister R, Eddy SR, et al. (2016). Epigenomic landscapes of retinal rods and cones. eLife 5, e11613. [PubMed: 26949250]

Money KM, and Stanwood GD (2013). Developmental origins of brain disorders: roles for dopamine. Front. Cell. Neurosci 7, 260. [PubMed: 24391541]

Prigge CL, Yeh PT, Liou NF, Lee CC, You SF, Liu LL, McNeill DS, Chew KS, Hattar S, Chen SK, and Zhang DQ (2016). M1 ipRGCs Influence Visual Function through Retrograde Signaling in the Retina. J. Neurosci 36, 7184–7197. [PubMed: 27383593]

Rao S, Chun C, Fan J, Kofron JM, Yang MB, Hegde RS, Ferrara N, Copenhagen DR, and Lang RA (2013). A direct and melanopsin-dependent fetal light response regulates mouse eye development. Nature 494, 243–246. [PubMed: 23334418]

Razafsky D, Blecher N, Markov A, Stewart-Hutchinson PJ, and Hodzic D (2012). LINC complexes mediate the positioning of cone photoreceptor nuclei in mouse retina. PLoS ONE 7, e47180. [PubMed: 23071752]

Renna JM, Weng S, and Berson DM (2011). Light acts through melanopsin to alter retinal waves and segregation of retinogeniculate afferents. Nat. Neurosci 14, 827–829. [PubMed: 21642974]

Renna JM, Chellappa DK, Ross CL, Stabio ME, and Berson DM (2015). Melanopsin ganglion cells extend dendrites into the outer retina during early postnatal development. Dev. Neurobiol 75, 935–946. [PubMed: 25534911]

Rich KA, Zhan Y, and Blanks JC (1997). Migration and synaptogenesis of cone photoreceptors in the developing mouse retina. J. Comp. Neurol 388, 47–63. [PubMed: 9364238]

Schiavo G, Benfenati F, Poulain B, Rossetto O, Polverino de Laureto P, DasGupta BR, and Montecucco C (1992). Tetanus and botulinum-B neurotoxins block neurotransmitter release by proteolytic cleavage of synaptobrevin. Nature 359, 832–835. [PubMed: 1331807]

Schmidt TM, Taniguchi K, and Kofuji P (2008). Intrinsic and extrinsic light responses in melanopsin-expressing ganglion cells during mouse development. J. Neurophysiol 100, 371–384. [PubMed: 18480363]

Sekaran S, Lupi D, Jones SL, Sheely CJ, Hattar S, Yau KW, Lucas RJ, Foster RG, and Hankins MW (2005). Melanopsin-dependent photoreception provides earliest light detection in the mammalian retina. Curr. Biol 15, 1099–1107. [PubMed: 15964274]

Semo M, Vugler AA, and Jeffery G (2007). Paradoxical opsin expressing cells in the inner retina that are augmented following retinal degeneration. Eur. J. Neurosci 25, 2296–2306. [PubMed: 17445228]

Siegert S, Cabuy E, Scherf BG, Kohler H, Panda S, Le Y-Z, Fehling HJ, Gaidatzis D, Stadler MB, and Roska B (2012). Transcriptional code and disease map for adult retinal cell types. Nat. Neurosci 15, 487–495, S1–S2. [PubMed: 22267162]

Sinagra M, Verrier D, Frankova D, Korwek KM, Blahos J, Weeber EJ, Manzoni OJ, and Chavis P (2005). Reelin, very-low-density lipoprotein receptor, and apolipoprotein E receptor 2 control somatic NMDA receptor composition during hippocampal maturation in vitro. J. Neurosci 25, 6127–6136. [PubMed: 15987942]

Sondereker KB, Onyak JR, Islam SW, Ross CL, and Renna JM (2017). Melanopsin ganglion cell outer retinal dendrites: Morphologically distinct and asymmetrically distributed in the mouse retina. J. Comp. Neurol 525, 3653–3665. [PubMed: 28758193]

Szabo, Szabo A, Enzso¨ ly A, Szél A, and Luka´ ts A(2014). Immunocytochemical analysis of misplaced rhodopsin-positive cells in the developing rodent retina. Cell Tissue Res. 356, 49–63. [PubMed: 24496510]

Tian N, and Copenhagen DR (2001). Visual deprivation alters development of synaptic function in inner retina after eye opening. Neuron 32, 439–449. [PubMed: 11709155]

Tian N, and Copenhagen DR (2003). Visual stimulation is required for refinement of ON and OFF pathways in postnatal retina. Neuron 39, 85–96. [PubMed: 12848934]

Tissir F, and Goffinet AM (2003). Reelin and brain development. Nat. Rev. Neurosci 4, 496–505. [PubMed: 12778121]

Toriyama M, Mizuno N, Fukami T, Iguchi T, Toriyama M, Tago K, and Itoh H (2012). Phosphorylation of doublecortin by protein kinase A orchestrates microtubule and actin dynamics to promote neuronal progenitor cell migration. J. Biol. Chem 287, 12691–12702. [PubMed: 22367209]

Tu DC, Zhang D, Demas J, Slutsky EB, Provencio I, Holy TE, and Van Gelder RN (2005). Physiologic diversity and development of intrinsically photosensitive retinal ganglion cells. Neuron 48, 987–999. [PubMed: 16364902]

Weber IP, Ramos AP, Strzyz PJ, Leung LC, Young S, and Norden C (2014). Mitotic position and morphology of committed precursor cells in the zebrafish retina adapt to architectural changes upon tissue maturation. Cell Rep. 7, 386–397. [PubMed: 24703843]

Yang MB, Rao S, Copenhagen DR, and Lang RA (2013). Length of day during early gestation as a predictor of risk for severe retinopathy of prematurity. Ophthalmology 120, 2706–2713. [PubMed: 24139125]

Yu J, Lei K, Zhou M, Craft CM, Xu G, Xu T, Zhuang Y, Xu R, and Han M (2011). KASH protein Syne-2/Nesprin-2 and SUN proteins SUN1/2 mediate nuclear migration during mammalian retinal development. Hum. Mol. Genet 20, 1061–1073. [PubMed: 21177258]

Zhang DQ, Wong KY, Sollars PJ, Berson DM, Pickard GE, and McMahon DG (2008a). Intraretinal signaling by ganglion cell photoreceptors to dopaminergic amacrine neurons. Proc. Natl. Acad. Sci. USA 105, 14181–14186. [PubMed: 18779590]

Zhang Y, Narayan S, Geiman E, Lanuza GM, Velasquez T, Shanks B, Akay T, Dyck J, Pearson K, Gosgnach S, et al. (2008b). V3 spinal neurons establish a robust and balanced locomotor rhythm during walking. Neuron 60, 84–96. [PubMed: 18940590]

Highlights

- Light acts via melanopsin retinal ganglion cells to restrict cones to their appropriate layer
- Ablation of melanopsin cells changes the cone photoreceptor transcriptome
- Dopamine signaling via the D4 receptor is a cue for cone positioning

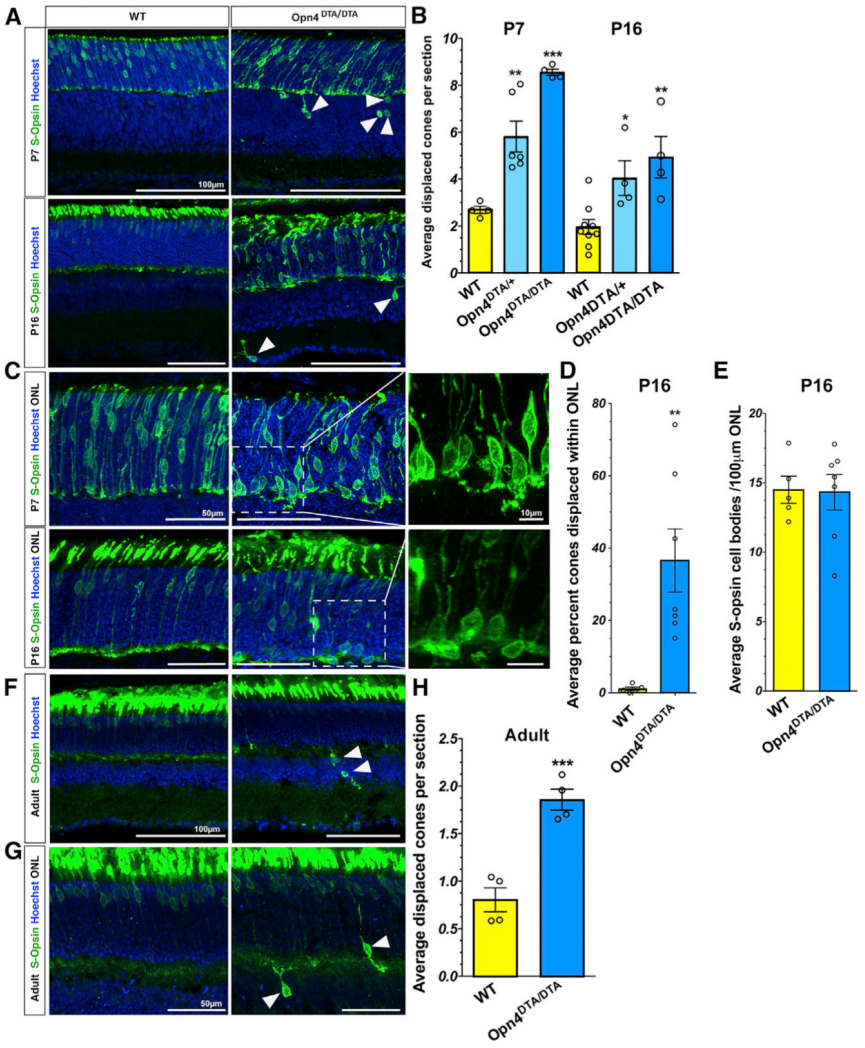

Figure 1. Ablation of ipRGCs Leads to Cone Lamination and Distribution Defects

(A) Representative images of retinal histological sections from P7 and P16 wild-type and *Opn4*$^{DTA/DTA}$ showing S-opsin-expressing DCs (arrowheads). Scale bar, 100 μm.

(B) Quantification of average number of DCs in wild-type, *Opn4*$^{DTA/+}$, and *Opn4*$^{DTA/DTA}$ retinas at P7 and P16. P7 wild-type (WT) n = 4, *Opn4*$^{DTA/+}$ n = 6, *Opn4*$^{DTA/DTA}$ n = 4; P16 WT n = 9, *Opn4*$^{DTA/+}$ n = 4, *Opn4*$^{DTA/DTA}$ n = 4; one-way ANOVA with Tukey's post-test. Average DCs per section (y axis) represents the number of DCs per histological section, which is on average 3,850 μm long at P7 (3,850 ± 227 μm, n = 3). Based on this measure and the total number of DCs/histological section (see Table S1), we estimate that there are 0.07 DCs/100 mm in wild-type and 0.22 DCs/100 mm in *Opn4*$^{DTA/DTA}$.

(C) S-opsin-immunostained retinal sections from wild-type and *Opn4*$^{DTA/DTA}$ retinas focused on the ONL (scale bar, 50 μm). Boxed area is shown magnified on the right (scale bar, 10 mm).

(D) Quantitation of the percent of cone somas displaced to the basal 50% of the ONL as a function of the total number of cone somas (WT 1.18 ± 0.47, n = 5; *Opn4*$^{DTA/DTA}$ 36.58 ± 8.73, n = 7; p = 0.007, Student's t test).

(E) Quantitation of total numbers of S-opsin cone somas per 100-μm retina in P16 wild-type versus *Opn4*$^{DTA/DTA}$ (WT 14.5 ± 0.98, n = 5; *Opn4*$^{DTA/DTA}$ 14.32 ± 1.28, n = 7; p = 0.92, Student's t test).

(F and G) Representative images of histological sections from adult (>P60) wild-type and *Opn4*$^{DTA/DTA}$ retinas at low (F) or high (G) magnification. Scale bar in F, 100 mm; scale bar in G, 50 μm.

(H) Quantification of average number of DCs in wild-type and *Opn4*$^{DTA/DTA}$ adult retinas. WT n = 4, *Opn4*$^{DTA/DTA}$ n = 4; p = 0.0004, Student's t test. See the Experimental Procedures for quantification details and total DC values. Data are repre-sented as mean ± SEM. See also Figures S1–S5 and Table S1.

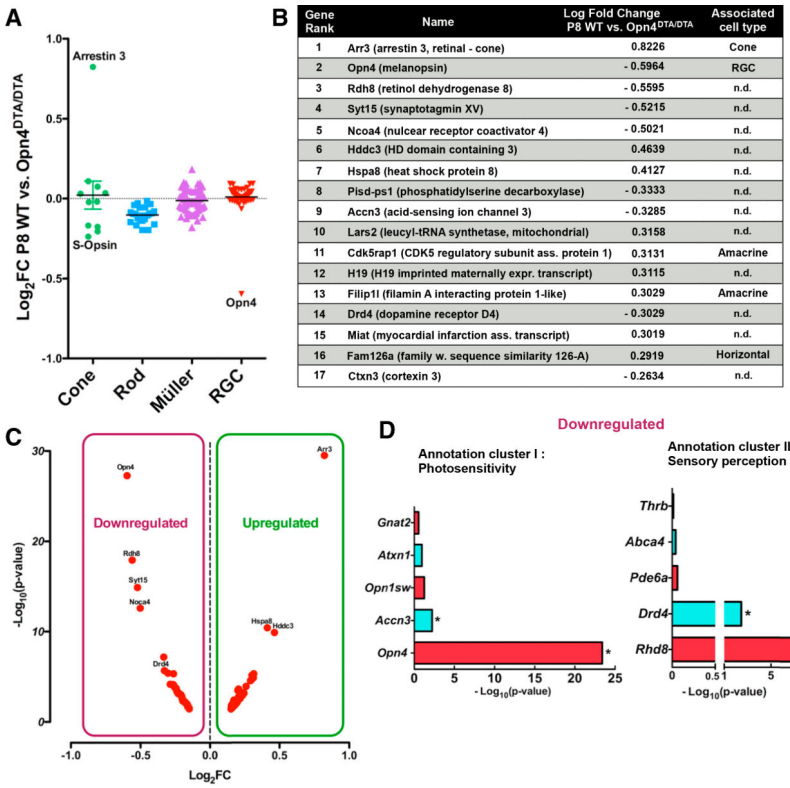

Gene Rank	Name	Log Fold Change P8 WT vs. Opn4$^{DTA/DTA}$	Associated cell type
1	Arr3 (arrestin 3, retinal - cone)	0.8226	Cone
2	Opn4 (melanopsin)	- 0.5964	RGC
3	Rdh8 (retinol dehydrogenase 8)	- 0.5595	n.d.
4	Syt15 (synaptotagmin XV)	- 0.5215	n.d.
5	Ncoa4 (nulcear receptor coactivator 4)	- 0.5021	n.d.
6	Hddc3 (HD domain containing 3)	0.4639	n.d.
7	Hspa8 (heat shock protein 8)	0.4127	n.d.
8	Pisd-ps1 (phosphatidylserine decarboxylase)	- 0.3333	n.d.
9	Accn3 (acid-sensing ion channel 3)	- 0.3285	n.d.
10	Lars2 (leucyl-tRNA synthetase, mitochondrial)	0.3158	n.d.
11	Cdk5rap1 (CDK5 regulatory subunit ass. protein 1)	0.3131	Amacrine
12	H19 (H19 imprinted maternally expr. transcript)	0.3115	n.d.
13	Filip1l (filamin A interacting protein 1-like)	0.3029	Amacrine
14	Drd4 (dopamine receptor D4)	- 0.3029	n.d.
15	Miat (myocardial infarction ass. transcript)	0.3019	n.d.
16	Fam126a (family w. sequence similarity 126-A)	0.2919	Horizontal
17	Ctxn3 (cortexin 3)	- 0.2634	n.d.

Figure 2. Ablation of ipRGCs Induces Transcriptional Changes in Cone Photoreceptors

(A) RNA sequencing performed on whole retinalextracts from P8 WT versus *Opn4*$^{DTA/DTA}$ animals with Log2 fold change (FC) change in expression level. Genes are assigned to cell type-specific categories using single-cell association rankings from retinal Drop-seq data in Macosko et al., 2015, with cone, rod, Müller and RGC categories shown. Individual points represent one cell type-specific gene.

(B) All significantly up- or downregulated genes inP8 WT versus *Opn4*$^{DTA/DTA}$ retinas with associated cell type category. n.d., category not determined.

(C) Volcano plot of all top differentially upand downregulated genes in P8 WT versus*Opn4*$^{DTA/DTA}$ retinas.

(D) DAVID gene functional annotation analysis of genes downregulated with a Log2 fold change greater than 0.15. Annotation cluster I photosensitivity, enrichment score 5.94; annotation cluster II sensory perception, enrichment score 2.33. See also Table S2.

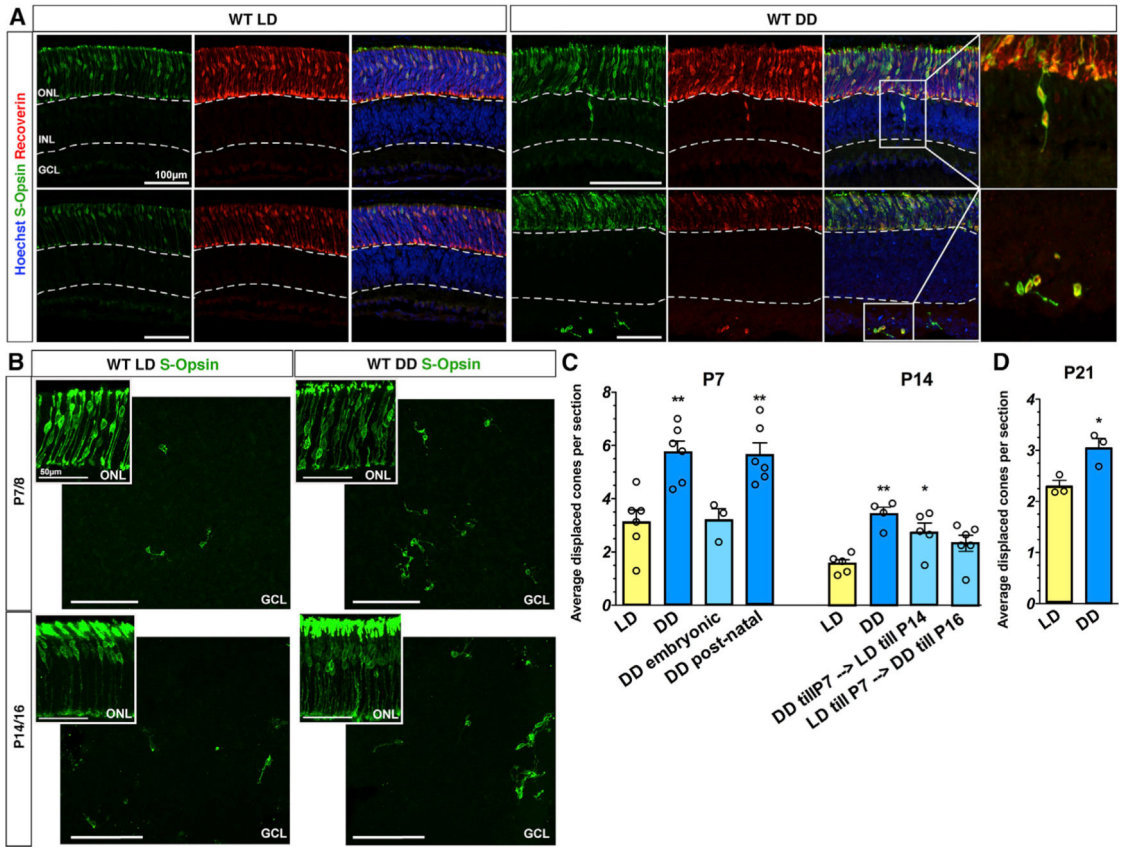

Figure 3. Visual Deprivation Displaces Cone Photoreceptors to Inner Retinal Layers

(A) Representative images of histological sections from wild-type light-reared (LD) and dark-reared (DD) animals at P7/P8 stained for the cone markers S-opsinand Recoverin. Scale bar, 100 μm.

(B) P7/P8 and P14/P16 retinal whole mounts from wild-type LD and DD animals stained with S-opsin. Images show DCs at the GCL level. Scale bar, 100 μm. Corresponding ONL cross-sections in insets show normal lamination of cones within the ONL of DD animals. Scale bar, 50 μm.

(C) The number of DCs observed at P7 or P14 after different light exposure conditions, as indicated. Data are represented as average number of DCs ± SEM per 20-μm retinal section (see the Experimental Procedures). P7: LD n = 6 versus DD n = 6 versus DD embryonic n = 5 versus DD post-natal n = 6; one-way ANOVA with Tukey's post-test. P14: LD n = 5 versus DD n = 5 versus DD until P7→LD until P14 n = 5 versus LD until P7→DD until P16 n = 5; one-way ANOVA with Tukey's post-test.

(D) DCs are increased in animals dark-reared until 21 days of age. P21: LD n = 3, DD n = 3; p = 0.016, paired Student's t test. See also Figure S6 and Table S1.

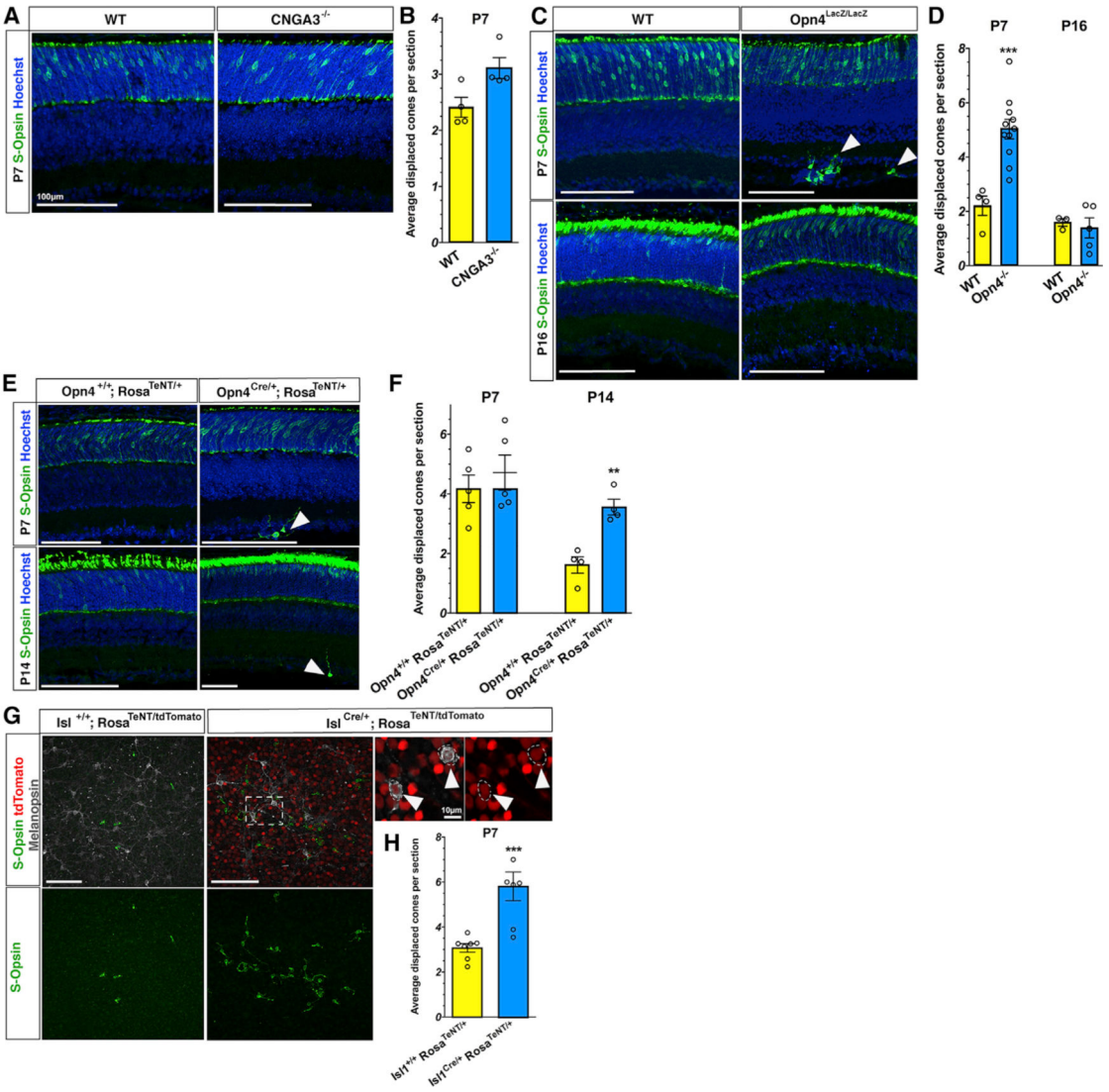

Figure 4. Cone Positioning Is Controlled by Activity in ipRGCs and Is Independent of Early Cone Phototransduction

(A) Representative images of histological sections from P7 wild-type and *Cnga3*$^{-/-}$ retinas immunostained for S-opsin.

(B) Quantification of the number of DCs in wild-type and *Cnga3*$^{-/-}$ retinas. The number of DCs is not significantly affected in the P7 *Cnga3*$^{-/-}$ retina versus control, although a trend toward an increase in DCs was observed (wild-type n = 4, *Cnga3*$^{-/-}$ n = 4; p = 0.11, Student's t test).

(C) Representative images of histological sections from P7 and P16 Opn4 knockout (*Opn4*$^{-/-}$ or *Opn4*$^{LacZ/LacZ}$) and wild-type littermates immunostained for Sopsin, showing DCs (arrowheads) in *Opn4*$^{LacZ/LacZ}$ retinas.

(D) An increase in the average number of DCs is observed in the P7 *Opn4*$^{LacZ/LacZ}$ versus control (wild-type n = 4, *Opn4*$^{LacZ/LacZ}$ n = 11; p = 0.0004, Student's t test), but not in the P16 *Opn4*$^{LacZ/LacZ}$ (wild-type n = 3, *Opn4*$^{LacZ/LacZ}$ n = 4; p = 0.35, Student's t test).

(E) Representative images of histological sections from P7 and P14/P16 *Opn4*$^{+/+}$; *Rosa*$^{TeNT/+}$ (control) and *Opn4*$^{Cre/+}$; *Rosa*$^{TeNT/+}$ retinas immunostained for S-opsin, showing DCs in the *Opn4*$^{Cre/+}$; *Rosa*$^{TeNT/+}$ (arrowheads).
(F) Quantification of DCs in controls and *Opn4*$^{Cre/+}$; *Rosa*$^{TeNT/+}$ at P7 and P14. P7: *Opn4*$^{+/+}$; *Rosa*$^{TeNT/+}$ n = 5, *Opn4*$^{Cre/+}$; *Rosa*$^{TeNT/+}$ n = 5; p = 0.22, Student's t test; P14: *Opn4*$^{+/+}$; *Rosa*$^{TeNT/+}$ n = 4, *Opn4*$^{Cre/+}$; *Rosa*$^{TeNT/+}$ n = 4; p = 0.002, Student's t test.
(G) Whole-mount retinas focused on the GCL from P7 *Isl1*$^{+/+}$; *Rosa*$^{TeNT/tdTomato}$ and *Isl1*$^{Cre/+}$; *Rosa*$^{TeNT/tdTomato}$ animals stained with melanopsin and S-opsin. All melanopsin-positive cells examined also co-expressed Isl1, as assessed by tdTomato expression (arrowheads in zoom inset from boxed area).
(H) Quantification of the number of DCs at P7 in *Isl1*$^{+/+}$; *Rosa*$^{TeNT/tdTomato}$ and *Isl1*$^{+/+}$; *Rosa*$^{TeNT/tdTomato}$ animals. *Isl1*$^{+/+}$; *Rosa*$^{TeNT/tdTomato}$ n = 7, *Isl1*$^{+/+}$; *Rosa*$^{TeNT/tdTomato}$ n = 7; p = 0.0007, Student's t test. Scale bars in A, C, E, and G, 100 μm; scale bar in G zoom inset, 10 μm. Data are represented as mean ± SEM. See also Figure S7 and Table S1.

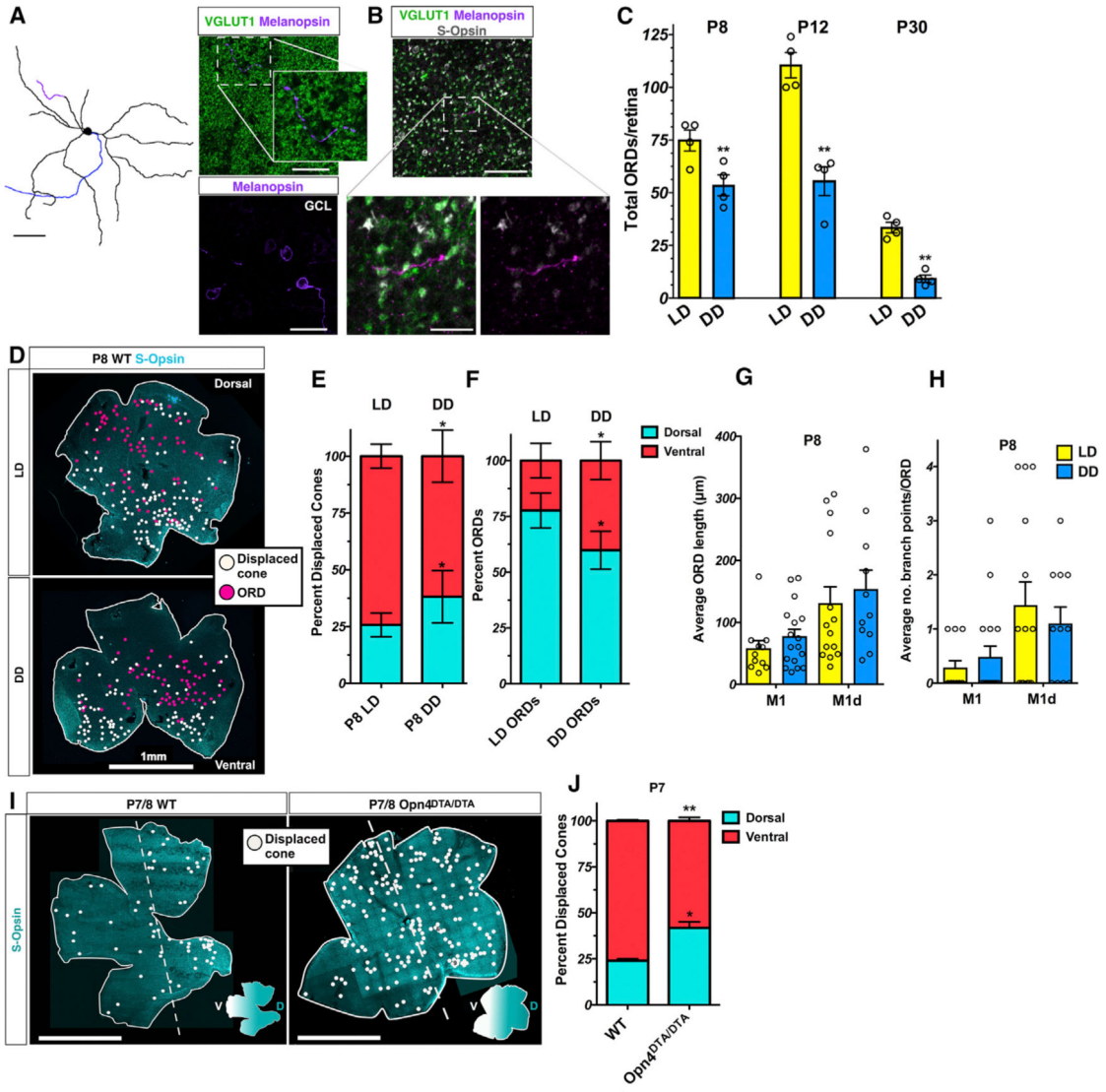

Figure 5. Visual Deprivation Decreases ipRGC ORDs, Increases DCs, and Disrupts Their Asymmetric Distribution

(A) A traced melanopsin ipRGC with ORD (purple) and axon (blue) indicated. Right panel shows whole mount of the same ipRGC ORD stained for VGLUT1 (photoreceptor terminals) and melanopsin, with the ORD shown in the inset.

(B) Additional ORD example showing co-localization of melanopsin-expressing ORD with S-opsin and VGLUT1. Scale bars, 50 µm.

(C) Counts of total number of ORDs at different ages in LD versus DD animals (mean ± SEM).

(D) Stitched reconstructions of melanopsin ORD gradients from retinal whole mounts at P8 in wild-type LD versus DD animals with locations of ORDs indicated (pink circles) and DCs (white circles).

(E and F) Proportion of DCs (E) and ORDs (F) located to the dorsal versus ventral retina in LD versus DD wild-type animals at P8 (mean ± SD).

(G) Quantification of M1 and M1d ORD length in P8 LD versus DD retinas (mean ± SEM).

(H) Quantification of number of M1 and M1d ORD branchpoints in P8 LD versus DD retinas (mean ± SEM).
(I) Stitched reconstructions of s-opsin-stained retinal whole mounts from wild-type and P8 *Opn4*$^{DTA/DTA}$ animals with locations of DCs (white circles).
(J) P7 *Opn4*$^{DTA/DTA}$ animals exhibited a significantly altered D/V distribution of DCs (mean ± SD). Whole-mount scale bars, 1 mm. See also Table S3.

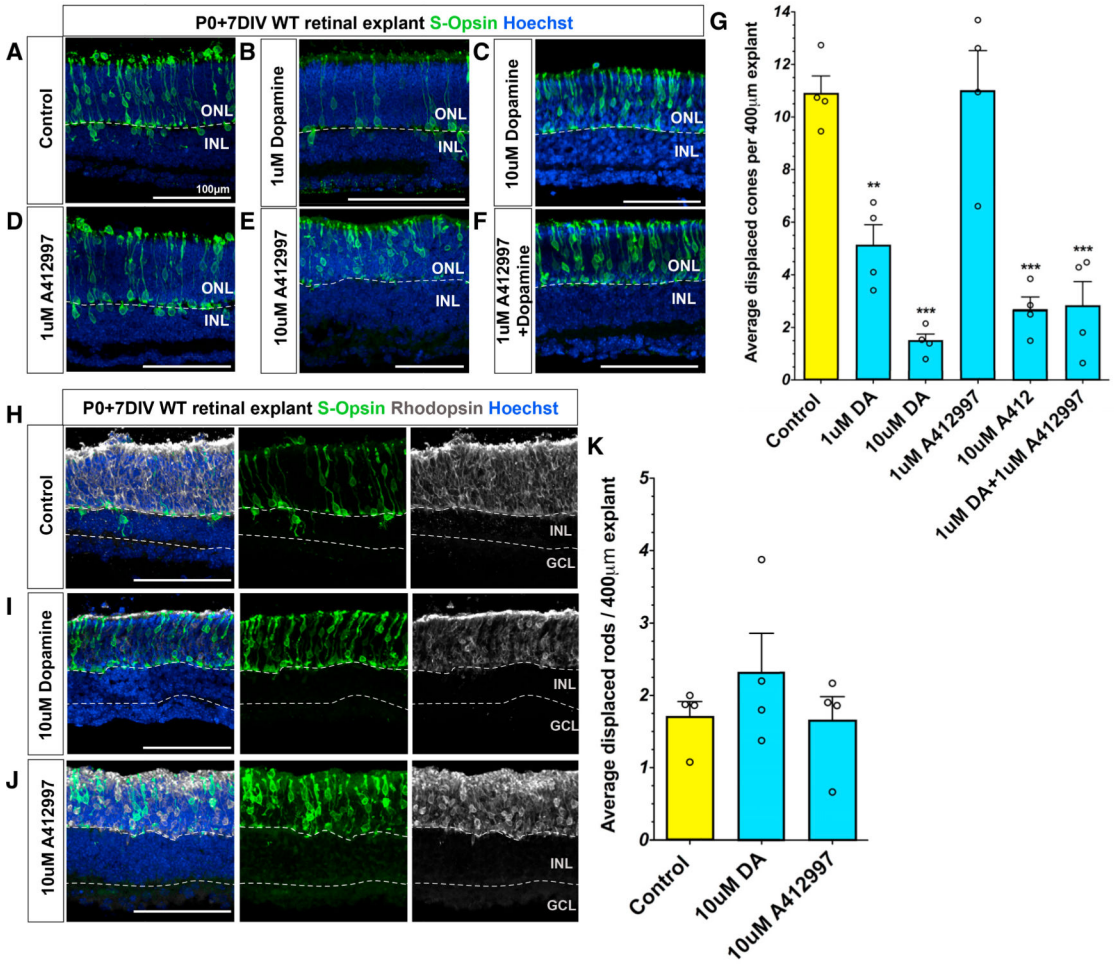

Figure 6. DA Administration Rescues Cone Lamination Defects in Retinal Explants

(A–F) Images of cross-sections from wild-type retinal explants prepared from P0 animals. Explants were treated with control media (A), 1 μM (B) or 10 μM (C) DAHCl, 1 μM (D) or 10 μM (E) D4 receptor agonist A412997, or a combination of 1 μM A412997 and DA (F). Dotted line indicates explant outer plexiform layer, the division between ONL and INL.

(G) Quantification of average number of cones displaced out of the ONL per 400-μm explant. Control, 10.88 ± 0.68 DCs; 1 μM A412997, 10.96 ± 1.56; 10 μM A412997, 2.5 ± 0.54; 1 μM DA, 5.1 ± 0.8; 10 μM DA, 1.47 ± 0.28; 1 μM A412997 + 1 μM DA, 2.8 ± 0.94; all conditions n = 4 independent experiments with 20 explant areas quantified per condition; one-way ANOVA with Tukey's post-test.

(H–J) Representative images of explants stained for S-opsin and Rhodopsin in explants treated with control media (H), 10 mM DA (I), or 10 mM A412997 (J).

(K) No significant changes were observed in the numbers of rods displaced out of the explant ONL. Control, 1.7 ± 0.21 displaced rods per 400-mm explant; 10 μM DA, 2.31 ± 0.54 displaced rods; 10 μM A412997, 1.65 ± 0.33 displaced rods; n = 4; p = 0.44, one-way ANOVA. Data are represented as mean displaced cells per 400-μm explant ± SEM. Scale bars, 100 μm. **p < 0.01 and ***p < 0.001. See also Figure S8.

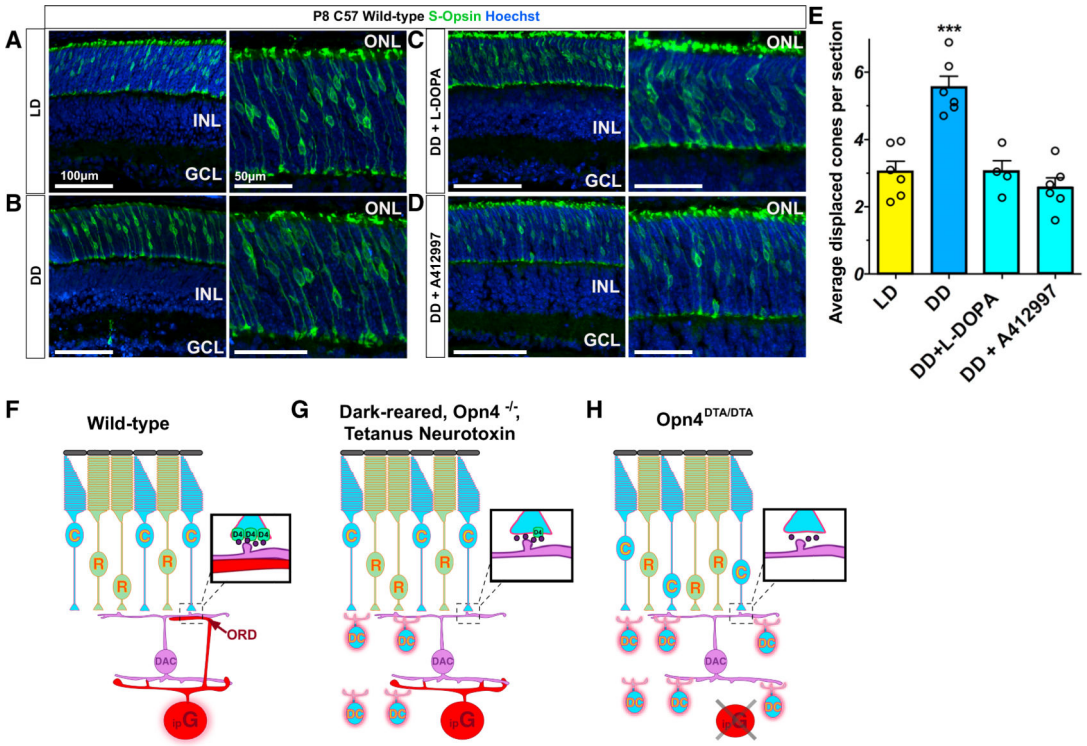

Figure 7. DA Administration Rescues the Effect of Developmental Dark Rearing In Vivo

(A–D) Representative images of histological sections from P8 light-dark (LD) control (A), uninjected dark-reared (DD) (B), L-DOPA-injected (C), or A412997injected (D) pups *in vivo* between P2 and P6. Augmenting DA signaling in DD pups restored the number of DCs (arrowhead) to that of LD controls. Scale bars, 100 and 50 03bcm (ONL inset).

(E) Quantification of average numbers of DCs in *in vivo* conditions (P8 LD n = 6, DD n = 6, DD + L-DOPA n = 4, DD + A412997 n = 6; one-way ANOVA).

(F–H) Proposed model of the interaction between ipRGCs and cones.

(F) In wild-type animals, light-evoked activity in ipRGCs (ipG) stimulates dopaminergic amacrine cells (DAC) via their ORDs to influence DA reception in conephotoreceptors (C) through the DA D4 receptor (D4), resulting in cones being repelled from the basal layers.

(G) In *Opn4*$^{-/-}$, dark-reared, or TeNT-expressing ipRGCs, light-evoked activity is decreased, leading to a reduced number of ORDs, reduced activation of DACs, and reduced DRD4 activation in cones, leading to cone displacement from the ONL (DCs).

(H) In *Opn4*$^{DTA/DTA}$ retinas, contacts between ipRGCs and DACs are abolished and DRD4 expression is significantly reduced, leading to more DCs in the inner retina as well as displacement of cones to the basal part of the ONL. Rod (R) positions are not affected. Data are represented as mean ± SEM. *p < 0.05, **p < 0.01, and ***p < 0.001. See also Table S1.